

A semi-mechanistic model for predicting daily variations in species-level live fuel moisture content

Rodrigo Balaguer-Romano^{a,b,*}, Rubén Díaz-Sierra^a, Miquel De Cáceres^c,
 Àngel Cunill-Camprubí^d, Rachael H. Nolan^e, Matthias M. Boer^e, Jordi Voltas^{d,f},
 Víctor Resco de Dios^{d,f,g}

^a Mathematical and Fluid Physics Department, Faculty of Sciences, Universidad Nacional de Educación a Distancia (UNED), Madrid 28040, Spain

^b EIUNED, Escuela Internacional de Doctorado. PhD Program in Sciences, Universidad Nacional de Educación a Distancia (UNED), Madrid 28040, Spain

^c CREAM, E08193 Bellaterra (Cerdanyola del Vallès), Catalonia, Spain

^d Joint Research Unit CTFC – AGROTECNIO – CERCA, Av. Alcalde Rovira Roure 191, Lleida 25198, Spain

^e Hawkesbury Institute for the Environment, Western Sydney University, Locked Bag 1797, Penrith, NSW 2751, Australia

^f Department of Crop and Forest Sciences, Universitat de Lleida, Lleida 25198, Spain

^g School of Life Science and Engineering, Southwest University of Science and Technology, Mianyang 621010, China

ARTICLE INFO

Key words:
 Wildfire
 Fire behaviour
 Drought stress
 Drought Code
 Remote sensing
 Phytophysiology

ABSTRACT

Live Fuel Moisture Content (LFMC) is one of the main factors affecting forest ignitability as it determines the availability of existing live fuel to burn. Currently, LFMC is monitored through spectral vegetation indices or inferred from meteorological drought indices. While useful, neither approach provides mechanistic insights into species-specific LFMC variation and they are limited in the ability to forecast LFMC under altered future climates. Here, we developed a semi-mechanistic model to predict daily variation in LFMC across woody species from different functional types by adjusting a soil water balance model which estimates predawn leaf water potential (Ψ_{pd}). Our overarching goal was to balance the trade-off between biological realism, which enhances model applicability, and parameterization complexity, which may limit its value within operational settings. After calibration, model predictions were validated against a dataset comprising 1659 LFMC observations across peninsular Spain, belonging to different functional types and from contrasting climates. The overall goodness of fit for our model ($R^2 = 0.5$) was better than that obtained by an existing models based on drought indices ($R^2 = 0.3$) or spectral vegetation indices ($R^2 = 0.1$). We observed the best predictive performance for seeding shrubs ($R^2 = 0.6$) followed by trees ($R^2 = 0.5$) and resprouting shrubs ($R^2 = 0.4$). Through its relatively simple parameterization, the approach developed here may pave the way for a new generation of process-based models that can be used for operational purposes within fire risk mitigation scenarios.

1. Introduction

Wildfires are a natural component of many terrestrial ecosystems, but they are becoming an increasing threat to civil protection, public health and national security worldwide (Borchers-Arriagada et al., 2021; Duane et al., 2021; Karavani et al., 2018; McDonald, 2020; Resco de Dios and Nolan, 2021; Tedim et al., 2020). Sustainable wildfire management should not seek to eliminate all fires in ecosystems that are naturally fire-prone. Instead, the target for wildfire management lies in

creating fuel structures, from local to landscape scales, that reduce the risk for life and property while maintaining ecological functions. In this context, a key aspect for fire prevention and management actions is understanding the temporal changes that occur in the moisture content of both, dead and live fuels. Wildfires can only occur once critical fuel dryness thresholds are crossed (Jurdao et al., 2012; Luo et al., 2019; Nolan et al., 2016), and management can significantly alter fuel growth and provide a better knowledge of where and when live and dead fuels are in a critically dry state for assessing the risk of large wildfires

Abbreviations: LFMC, life fuel moisture content; Ψ_{pd} , predawn leaf water potential; Ψ_{soil} , soil water potential; DC, Drought Code; EVI, Enhanced Vegetation Index.

* Corresponding author at: Mathematical and Fluid Physics Department, Faculty of Sciences, Universidad Nacional de Educación a Distancia (UNED), Madrid 28040, Spain.

E-mail address: rodrigo.balaguer@ccia.uned.es (R. Balaguer-Romano).

<https://doi.org/10.1016/j.agrformet.2022.109022>

Received 10 December 2021; Received in revised form 17 May 2022; Accepted 22 May 2022

0168-1923/© 2022 The Author(s). Published by Elsevier B.V. This is an open access article under the CC BY license (<http://creativecommons.org/licenses/by/4.0/>).

(Moreno-Gutiérrez et al., 2011).

Wildfire activity depends on the interplay between biomass loads and connectivity along with the availability of such biomass to burn, which is strongly determined by moisture content (Boer et al., 2021). While dead fuel moisture content (DFMC) variations have been far researched (Matthews, 2014), there are significant knowledge gaps regarding live fuel moisture content (LFMC) variations that can be addressed from a plant physiology perspective. LFMC, the water content in live foliage and small twigs on a dry mass basis, critically affects forest ignitability and likelihood of fire spread (Balaguer-Romano et al., 2020; Gabriel et al., 2021; Pimont et al., 2019; Rossa, 2017). This is because the water content of live tissues acts as a heat sink, consequently reducing the intensity of fire and its rate of spread (Rothermel, 1983).

In forest ecosystems, where plant biomass is inherently abundant enough to sustain a fire, fire activity is primarily constrained by the frequency and duration of dry weather periods (Boer et al., 2021). In Mediterranean forests and shrublands, amongst other parts of the world, climate aridity is projected to increase during the 21st century as a result of global change (IPCC, 2021). Consequently, increasing water scarcity may lead to longer fire seasons and higher fire danger as LFMC distributions shift towards drier levels for long periods of time (Ma et al., 2021; Resco de Dios et al., 2021).

Many fire management agencies routinely monitor LFMC directly through time-consuming and expensive field inventories or indirectly through remote sensing products or meteorological drought indices. Remotely-sensed approaches, which include spectral vegetation indices and radiative transfer models, allow the monitoring of LFMC over large areas at fine spatial and temporal resolutions (Yebrá et al., 2013). Drought indices, such as the Drought Code (DC) from the Canadian Forest Fire Weather Index (Van Wagner, 1974), are based on daily air temperature and precipitation data and are designed to conceptually represent water dynamics in soil reservoirs. Common limitations to both indirect approaches are that they provide incomplete information on interspecific differences, at least without a priori calibrations, and that forecasting relies on empirical methods. Furthermore, a number of studies have cast doubt on the reliability of DC as an actual proxy of LFMC, at least in some plant functional types in the Mediterranean basin (Ruffault et al., 2018; Soler Martin et al., 2017).

The degree of variation in LFMC within a fire season varies markedly across life-forms, at least in Mediterranean environments (Resco de Dios, 2020). This variation arises from differences in physiological and anatomical characteristics controlling LFMC such as stomatal control, the degree of sclerophylly, or rooting depth (Sánchez-Martínez et al., 2020). Empirical studies have often observed how seasonal variation in LFMC is largest in seeding shrubs, intermediate in resprouting shrubs and lowest in trees (Nolan et al., 2018; Pellizzaro et al., 2007b; Viegas et al., 2001). Seeding shrubs often have shallow root systems which cannot reach deeper water sources (Nolan et al., 2018), high resistance to embolism (Pausas et al., 2016) and poor stomatal controls (Resco de Dios, 2020), which jointly lead to the lowest LFMC values during drought periods and the largest seasonal variation. Resprouting shrub species often have deeper roots and lower drought tolerance than seeders, leading to intermediate variation in LFMC (Resco de Dios, 2020). Tree species often have the deepest rooting systems and strong stomatal controls, which buffers against short term fluctuations in shallow water levels and, consequently, they often display nearly constant LFMC throughout the fire season (Nolan et al., 2018; Viegas et al., 2001).

Nolan et al. (2020) demonstrated that inter-species variation in LFMC could in principle be modelled as a function of predawn leaf water potential (Ψ_{pd}), given information on pressure-volume relationships. This approach can be further simplified and LFMC may be modelled from Ψ_{pd} using solely a linear regression when plants are operating below the turgor loss point, which is the most critical from the perspective of fire occurrence (Nolan et al., 2018). In a case study using six species from a Mediterranean forest, the prediction of LFMC from Ψ_{pd}

showed an overall goodness of fit that was better than that from existing drought indices (Nolan et al., 2018). To scale up from local to larger areas, LFMC predictions would require predictions of Ψ_{pd} which, in turn, is strongly related to rhizosphere soil water potential (Ψ_{soil}). That is, Ψ_{pd} overnight equilibrates with Ψ_{soil} in the absence of nocturnal transpiration or significant disruptions in the soil-plant-atmosphere continuum (Ritchie and Hinckley, 1975). However, to our knowledge, no study has yet attempted large scale LFMC modelling by coupling a soil water balance model with a physiological model.

MEDFATE is a forest ecosystem model designed to simulate soil and plant water balances in forest stands with heterogeneous structure and composition (De Cáceres et al., 2021, 2015). Aboveground stand structure is represented by total height, leaf area index and crown ratio of a set plant cohort. In MEDFATE, a plant cohort represents a set of plants that belong to the same species with similar structural characteristics, including root distribution, which is specified using the depths corresponding to cumulative 50% and 95% of fine roots. Soil is represented using a set of vertical layers with different depths and physical properties. Finally, the model requires daily weather data as inputs to simulate plant hydraulics and transpiration at subdaily time steps (De Cáceres et al., 2015).

Here we seek to develop a novel approach for forecasting daily variations in LFMC across Mediterranean species by merging soil and plant water potential simulations from MEDFATE (De Cáceres et al., 2021) with previously developed Ψ_{pd} -LFMC based models (Nolan et al., 2018). More specifically, we seek to model LFMC variation across species grouped in three functional types (seeding shrubs, resprouting shrubs and trees) from Ψ_{pd} values, and compare the results with current approaches such as the Drought Code and remotely sensed vegetation indices. To this end, we used the Spanish subset of a global LFMC database (Yebrá et al., 2019) for calibration and validation. Our ultimate goal was to develop an approach that can be used within operational settings. Considering the usual trade-off between the degree of biological realism that is incorporated into a model and how applicable and easy to use the model will be, we seek to merge simplicity with biological realism to enhance applicability by making some simplifying assumptions on the biological differences across species.

2. Materials and methods

2.1. Globe-LFMC database

Globe-LFMC is a global database of live fuel moisture content measured from 1383 sampling sites in 11 countries (Yebrá et al., 2019). Each individual record represents an *in situ* destructive measurement of LFMC. We selected all sites within Spain with species specific records, resulting in 40 sampling sites containing 2511 individual records with observed LFMC. Data includes 37 species (Methods A1) from 21 different genera covering a sampling period of 20 years from 1996 to 2017 (Table A1). Sampling sites cover many of the contrasting climates and ecoregions of peninsular Spain (Fig. 1).

Mean annual air temperature varied from 10.9 to 17.8 °C and mean annual precipitation from 243 to 1345 mm across the selected sampling sites (Fig. 1b, c, Table A1). Vegetation types and ecoregions ranged from xeric sclerophyll or Mediterranean pine forests to the more mesic Cantabrian mixed forests, dominated by temperate deciduous broad-leaf species (Fig. 1a).

2.2. MEDFATE

MEDFATE (version 2.2.3) is a process-based soil-vegetation-atmosphere transfer model implemented in an R package, which uses soil, vegetation, and meteorological data to predict soil moisture dynamics (De Cáceres et al., 2021; Table A2). The model is based on the BILJOU and SIERRA water balance models (Granier et al., 1999; Mouillot et al., 2001) and predicts, at a daily time steps, the soil water content as a

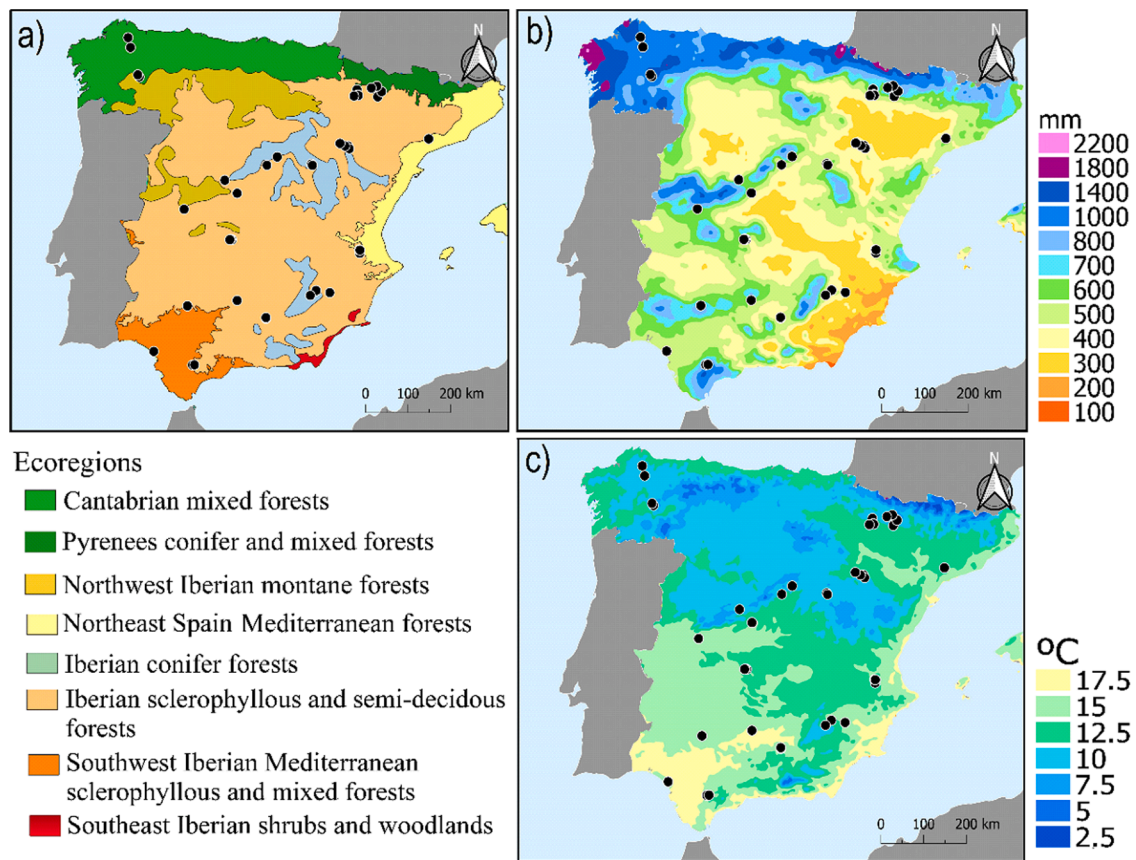


Fig. 1. Globe-LFMC sampling sites in Spain. (a) Ecoregions, (b) mean annual precipitation and (c) mean annual air temperature. Black circles indicate the location of our study sites. Ecoregions delimitations obtained from [Dinerstein et al. \(2017\)](#) and meteorological gradients from [Chazarra Bernabé et al. \(2018\)](#).

function of soil properties, stand structure and daily climatic variables. Thus, daily changes in soil water content are calculated as the difference between precipitation, the water input, and canopy interception, plant transpiration, bare soil evaporation, surface runoff and deep drainage ([De Cáceres et al., 2021, 2015](#)). Also, the model predicts daily plant transpiration and photosynthesis rates. Based on [Sperry et al. \(2017\)](#), stomatal regulation of gas exchange is simulated at sub-daily steps involving detailed calculations of hydraulics, leaf energy balance and photosynthesis.

We divided the soil into four layers (0–10 cm, 10–20 cm, 20–60 cm and 60–100 cm deep). When a given soil layer is filled, water percolates to the next layer below, except in the deepest layer where water is lost from the profile via deep drainage. Soil data inputs are bulk density, the percentage of clay, sand, organic matter and rock fragment content, which were derived from the Soil Grids System at 250 m resolution ([Hengl et al., 2017](#)). A previous sensitivity analysis has shown that modelled transpiration is more sensitive to meteorological or vegetation inputs such as annual rainfall and leaf area index (LAI) than to soil inputs such as soil depth of layers or soil texture variation from clayey soils to sandy soils ([De Cáceres et al., 2015](#)).

Vegetation data inputs are species identity, tree density, shrub cover, plant height, tree diameter at breast height and plant rooting depth. All data except rooting depth were obtained from the nearest plot which includes the target species from the Third National Forest Inventory of Spain ([Alberdi et al., 2016](#)), following the same approach as in previous publications ([De Cáceres et al., 2021](#)). MEDFATE requires the rooting depth where the cumulative 50% (Z50) and 95% (Z95) of fine roots occur. Previous studies have incorporated species-specific differences from a model assuming that vegetation is at eco-hydrological equilibrium ([Cabon et al., 2018](#)). However, to simplify model parameterization and diminish computational demands, we assumed that Z50 and Z95

occurred at 10 cm and 20 cm for seeding shrubs (R-), at 20 cm and 75 cm for resprouting shrubs (R+) and at 20 cm and 100 cm for trees (Tr), respectively. We chose these depths as they are consistent with previously defined soil depths and with our assumptions that seeding shrubs (R-) have shallow root systems that can only access shallow water resources; that tree (Tr) species have the deepest rooting systems and are able to extract water from superficial and also from deep layers; and that resprouting shrubs (R+) have an intermediate root distribution. MEDFATE also includes a set of species-specific plant traits covering plant size, shrub and tree allometric coefficients to predict biomass fuel loading, phenology and anatomy characteristics, tissue moisture, light extinction, transpiration, and photosynthesis ([De Cáceres et al., 2021](#)). We used the default values for each species with the aim of using a parsimonious parameterisation to enhance the potential application of the model.

Temperature, precipitation and wind speed were obtained for each sampling site (in a $0.1^\circ \times 0.1^\circ$ grid) from the ERA-5 Land reanalysis dataset ([Hersbach et al., 2020](#)), which provides hourly estimates of climate variables from the Copernicus Climate Change Service. Daily meteorological variables of relative humidity, incoming solar radiation, and potential evapotranspiration were then obtained using the *meteo-land* R package ([De Cáceres et al., 2018](#)). Relative humidity was estimated assuming that dew point temperature equals the minimum temperature, and potential solar radiation was estimated from latitude, slope and aspect. Incoming solar radiation was then obtained following [Thornton and Running \(1999\)](#).

Input data were then used to predict daily species-specific Ψ_{pd} values and simulations were ran with a one-year spin-up period to avoid interferences from initial conditions.

2.3. Model calibration and validation

We divided the Globe-LFMC database into a calibration and a validation dataset. The calibration dataset was obtained by randomly sampling amongst sites and species using 34% of the total dataset, that is, 852 data points. After obtaining Ψ_{pd} from MEDFATE, we calibrated its relationship with LFMC based on a linear regression where, following Nolan et al. (2018), Ψ_{pd} had been logarithmically transformed. We used a single relationship between LFMC and Ψ_{pd} for all species in the entire dataset, instead of using separate relationships for each species. This is because we sought to increase model simplicity within operational settings and because not all the species present in the dataset had enough measurements for independent calibration. The validation dataset, containing the remaining 1659 data points (representing 66% of the total), was used to validate the LFMC predictions. Model validation was performed by a linear regression between observed and predicted LFMC calculating the adjusted R-squared (R^2) to measure the goodness of fit of our predictions, as well as the intercept (β_0) and the slope (β_1), and their 95% confidence interval, to test for model prediction biases. We also calculated the root mean square error (RMSE) and the mean absolute error (MAE) to quantify the accuracy of the predictions, and the mean biased error (MBE; Jolliff et al., 2009) to assess if our predictions underpredict or overpredict observed data.

2.4. Drought indices and spectral vegetation indices

We compared the goodness of fit of our approach with predictions from existing drought indices and spectral vegetation indices using the same Globe-LFMC database validation dataset. We obtained Drought Code (DC) values using the Canadian Forest Fire Danger Rating System, as implemented in the *cffdrs* R package (Wang et al., 2017), using the same meteorological data sources as those previously described for MEDFATE, and also leaving a one year spin-up period to avoid interference from initial conditions.

Following Marino et al. (2020), we calculated nine spectral indices (Table A3) to infer LFMC using data from the Moderate Resolution Imaging Spectrometer (MODIS) MCD43A4 Collection 6 reflectance product produced acquired daily tiles at 500-metre resolution. Data was downloaded from the NASA Land Processes Distributed Active Archive center (LP DAAC, <https://lpdaac.usgs.gov/>). Then, for each sampling date and site we extracted the values of each MODIS band as a simple pixel extraction which corresponded with the sampling site area. We regressed the spectral indices against observed LFMC to select the index with the highest adjusted R^2 in subsequent analyses (Enhanced Vegetation Index (EVI), $R^2=0.33$, Fig. A1). As EVI values included all the species present in the sampling site area, we additionally calculated the equivalent water thickness (EWT) from individual LFMC values to enhance comparability. EWT, which is a measure of water content per unit surface area of the vegetation (Sow et al., 2013), was calculated following Chakroun et al. (2015):

$$EWT = \frac{1}{\rho_w} \frac{1}{N} \sum (LFMC_i) \left(\frac{1}{SLA_i} \right) \quad (1)$$

where LFMC is the observed foliar moisture content recorded in the Globe-LFMC database, ρ_w is the density of pure water (1000 kg m^{-3}) and SLA is the specific leaf area. Species-specific SLA values were obtained from the MEDFATE plant traits set. We calculated the EWT of N species contained in each study site for each sampling date by applying Eq. (1) for i species. Finally, as vegetation index signals saturate in the upper ranges, EVI values were logarithmically transformed before regression against EWT.

2.5. Statistical analysis

To assess for significant differences across the approaches used for

calibration, we used an encompassing test of Davidson and MacKinnon (1993) with the “*lmtest*” R package (Zeileis and Hothorn, 2002). To compare two non-nested models, the test fits a third encompassing model which contains all regressors from both models. Then, the *encomptest()* function performs a Wald test for comparing each models against the encompassing model. If there are significant differences between each linear model against the encompassing model, the test indicates that both linear models are significantly different.

3. Results

The dataset allowed for model testing and calibration under a wide range of LFMC values, which varied across functional groups as expected. That is, LFMC variation was largest in seeding shrubs (45–145%, 5 and 95% percentiles, respectively), and intermediate in resprouting shrubs (60–120%). Average variations in trees (75–140%) were larger than in shrubs due to physiological differences between *Pinus* and *Quercus*, although seasonal variations within each genus were smaller than those obtained for seeders and resprouters. Across all species and years, the average seasonal values varied between 125% in spring to 80% in summer.

3.1. Calibration, validation and comparison of MEDFATE, dc and EVI

Using the calibration dataset, we regressed predicted Ψ_{pd} (logarithmically transformed), and DC values against observed LFMC, and EVI (logarithmically transformed) against the equivalent water thickness (EWT) (Fig. A2). The encompassing test of Davidson and MacKinnon showed significant differences ($p < 0.001$) in the predictions of LFMC based on MEDFATE and on DC, against the encompassing model which contains all regressors from both models. Our model showed significantly better fit than DC (Fig. A2). EVI could not be included in this analysis as the response variables were different (LFMC vs EWT). Then, the equations derived from these linear regressions were subsequently applied to Ψ_{pd} , DC and EVI values obtained for the validation dataset. LFMC predictions using our approach ($MEDFATE_{LFMC}$) showed a substantial improvement over those based on the drought index (DC_{LFMC}) and the spectral vegetation (EVI_{EWT}) index (Table 1, Fig. 2).

The overall goodness of fit of our model, $MEDFATE_{LFMC}$ (R^2 of observed against predicted LFMC relationship of 0.5), was better than for DC_{LFMC} ($R^2 = 0.3$) or EVI_{EWT} ($R^2=0.1$). The RMSE and MAE in our model (31 and 22%, respectively) were also smaller than in DC_{LFMC} (34 and 24%, respectively). It is worth noting that the goodness of fit in DC_{LFMC} depended on the functional type. That is, DC_{LFMC} showed a reasonable performance ($R^2 = 0.5$) for seeding shrubs (Fig. 2h), albeit lower than in our model ($R^2 = 0.6$, Fig. 2c). However, neither DC_{LFMC} nor EVI_{EWT} were reliable predictors of LFMC or EWT respectively as the coefficients of determination in resprouting shrubs or trees were lower than $R^2 = 0.2$ in all cases (Fig. 2).

3.2. $MEDFATE_{LFMC}$ features

Despite the improvement of $MEDFATE_{LFMC}$ over DC_{LFMC} and EVI_{EWT} , it is worth noting that our approach tended towards underprediction, particularly in the upper range of LFMC values (Fig. 2, Table 1). We observed that the slope of the observed vs predicted regression was 1.4 and the MBE was -8.8% , indicating this tendency towards underprediction. Our approach showed better goodness of fit for seeding shrubs ($R^2=0.6$, MAE =21%) than for trees ($R^2=0.5$, MAE =23%) or resprouting shrubs ($R^2=0.4$, MAE =21%). Also, we observed that MBE was lower for seeding shrubs (-5%) than for resprouters (-13%) or trees (-16% ; Table 1). Predictions of LFMC from $MEDFATE_{LFMC}$ realistically captured the differences in temporal patterns of moisture content (Fig. A3), across genus (Table 2) and species (exemplified in Fig. 3).

The performance of the $MEDFATE_{LFMC}$ model generally increased when examining variations at the genus level. We observed the best

Table 1

Goodness of fit statistics for the three approaches used in this study: $MEDFATE_{LFMC}$, Drought Code (DC_{LFMC}) used to predict LFMC, and Enhanced Vegetation Index (EVI_{EWT}) used to predict EWT, for each functional type (R-, seeding shrubs; R+, resprouting shrubs; Tr, trees). We calculated the adjusted R-squared (R^2), the intercept (β_0), and the slope (β_1), with each standard error in brackets, of the regression between observed and predicted LFMC, and also the root mean square error (RMSE), mean absolute error (MAE) and mean biased error (MBE) and the 95% confidence interval for correlation coefficients (CI_{low} and CI_{up}).

	R^2	β_0	β_1	RMSE	MAE	MBE	CI_{low}	CI_{up}
$MEDFATE_{LFMC}$	0.5	-25.4 (± 3.1)	1.4 (± 0.0)	31.1	22.3	-8.8	1.3	1.4
R-	0.6	-28.9 (± 3.4)	1.4 (± 0.0)	28.7	21.5	-4.8	1.3	1.4
R+	0.4	-22.1 (± 12.1)	1.4 (± 0.1)	32.4	21.4	-12.9	1.1	1.6
Tr	0.5	-22.7 (± 7.7)	1.4 (± 0.1)	34.7	22.7	-15.8	1.2	1.6
DC_{LFMC}	0.3	-6.2 (± 3.7)	1.1 (± 0.0)	33.6	24.3	-3.4	1.0	1.2
R-	0.5	-46.7 (± 4.3)	1.5 (± 0.0)	31.3	23.4	-4.6	1.5	1.6
R+	0.07	49.5 (± 5.9)	0.4 (± 0.1)	31.2	22.5	6.5	0.3	0.5
Tr	0.09	44.2 (± 11.1)	0.7 (± 0.1)	41.6	29.5	-14.6	0.5	1.0
EVI_{EWT}	0.1	-0.001 (± 0.0)	1.0 (± 0.0)	0.005	0.003	-0.0002	0.9	1.2
R-	0.1	0.001 (± 0.0)	0.7 (± 0.0)	0.002	0.001	0.0004	0.6	0.9
R+	0.2	-0.001 (± 0.0)	0.9 (± 0.1)	0.004	0.003	0.0004	0.8	1.3
Tr	0.03	-0.004 (± 0.0)	0.9 (± 0.4)	0.01	0.008	-0.0002	0.4	1.4

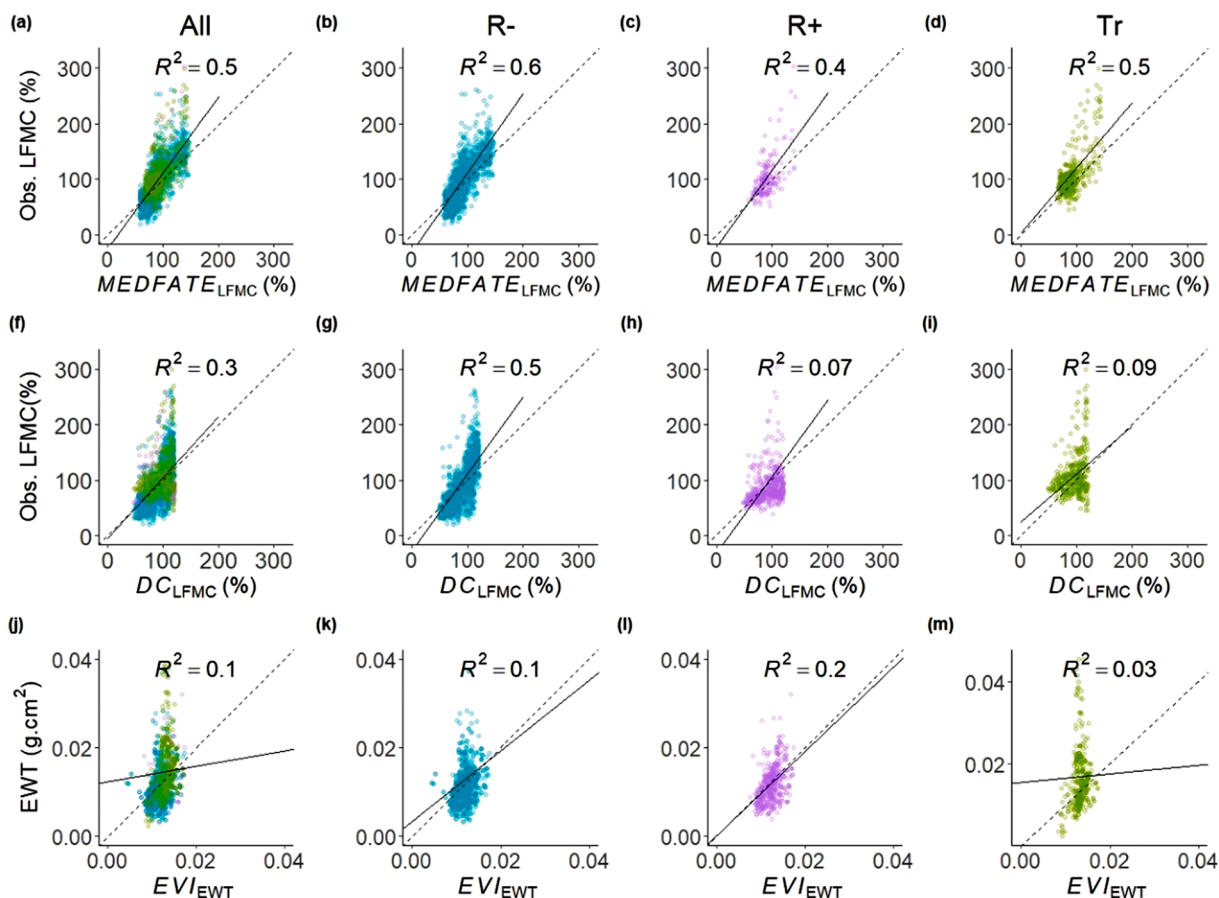


Fig. 2. Observed LFMC against predicted values from $MEDFATE_{LFMC}$ (a-d) and Drought Code (DC_{LFMC} ; f-i), and Equivalent Water Thickness against Enhanced Vegetation Index (EVI_{EWT} ; j-m) for all the data (a, f, j) or separately across functional types of seeding shrubs (R-; b, g, k) in blue, resprouting shrubs (R+; c, h, l) in purple and trees (Tr; d, i, m) in green. The line and the R^2 indicate the results of least squares fitting.

goodness of fit across seeding genera like *Cistus* ($R^2 = 0.7$, MAE = 16%), *Thymus* ($R^2 = 0.7$, MAE = 34%), *Salvia* ($R^2 = 0.6$, MAE = 24%), *Lavandula* ($R^2 = 0.5$, MAE = 53%) and *Ulex* ($R^2 = 0.5$, MAE = 20%). We observed a higher β_1 for *Thymus* (3.9) and *Lavandula* (3.0), indicating stronger underprediction of the model, but the slope remained between 1.1–1.5 for the other seeder shrubs. LFMC predictions for the two tree genera, *Pinus* and *Quercus*, showed an $R^2 = 0.6$ (*Quercus*) and $R^2 = 0.5$ (*Pinus*) and MAE between 37% (*Quercus*) and 17% (*Pinus*). For resprouting shrubs, we observed a larger variation in goodness of fit, as the coefficient of correlation ranged from $R^2 = 0.3$ in *Erica* (MAE =

18%), to $R^2 = 0.5$ in *Arbutus* (MAE = 50%), $R^2 = 0.5$ in *Buxus* (MAE = 11%) and $R^2 = 0.6$ in *Genista* (MAE = 20%).

4. Discussion

We developed, calibrated and validated a novel approach to predict daily values of LFMC across different species after modelling Ψ_{pd} using a plant-soil water balance model. Our approach keeps a compromise between being mechanistic and operational, as it makes a series of simplifying assumptions on the rooting depth parameters which drive,

Table 2

Goodness of fit statistics for each genus LFMF predicted with $MEDFATE_{LFMC}$. Sample size (n), adjusted R-squared (R^2), intercept (β_0) and slope (β_1), with each standard error in brackets, from regressing observed against predicted LFMF for all the data, and also separately for each functional type and each genus (when $n > 20$). We also show the root mean squared error (RMSE), mean absolute error (MAE), and mean bias error (MBE) and the 95% confidence interval for correlation coefficients (CI_{low} and CI_{up}).

	n	R^2	β_0	β_1	RMSE	MAE	MBE	CI_{low}	CI_{up}
Cistus (R-)	483	0.7	-5.3 (± 3.5)	1.1 (± 0.0)	20.7	16.1	-5.4	1.0	1.2
Lavandula (R-)	33	0.5	-149.6 (± 50.6)	3.0 (± 0.6)	68.4	52.9	-34.2	1.9	4.2
Salvia (R-)	473	0.6	-43.2 (± 5.3)	1.5 (± 0.1)	30.1	24.0	-5.6	1.4	1.6
Thymus (R-)	47	0.7	-251.2 (± 31.3)	3.9 (± 0.4)	41.8	33.6	4.9	3.2	4.7
Ulex (R-)	46	0.5	-19.4 (± 23.1)	1.1 (± 0.3)	24.2	20.5	10.7	0.6	1.7
Arbutus (R+)	29	0.5	-24.3 (± 37.9)	1.7 (± 0.3)	62.1	50.5	-49.1	1.0	2.4
Buxus (R+)	53	0.4	53.4 (± 12.5)	0.5 (± 0.1)	13.2	11.3	-4.3	0.2	0.7
Erica (R+)	43	0.3	4.5 (± 18.1)	0.9 (± 0.2)	21.2	17.6	3.4	0.5	1.3
Genista (R+)	30	0.6	-71.1 (± 22.7)	1.7 (± 0.3)	22.8	19.4	11.8	1.2	2.3
Pinus (Tr)	121	0.5	64.4 (± 16.9)	0.4 (± 0.2)	20.5	16.8	-7.2	0.1	0.7
Quercus (Tr)	347	0.6	-28.2 (± 7.9)	1.5 (± 0.1)	36.4	23.1	-17.5	1.3	1.7

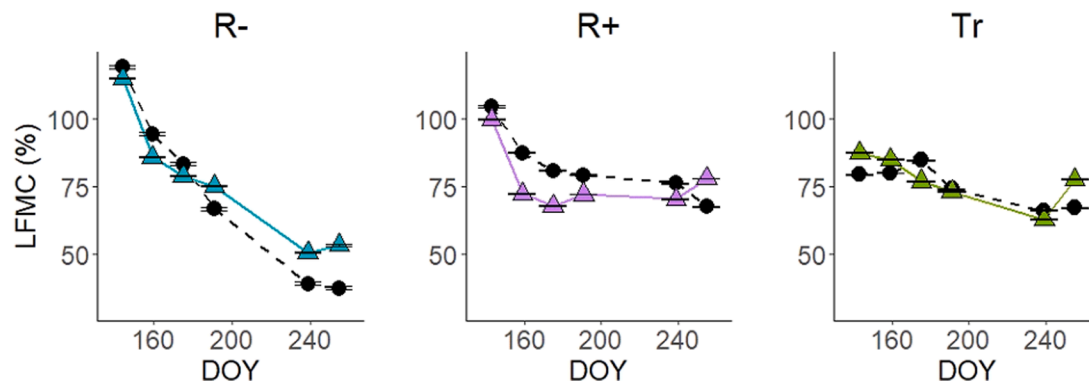


Fig. 3. Observed (black dashed line) and $MEDFATE_{LFMC}$ predicted (colour continuous line) LFMF seasonal dynamics across functional types, including a seeder (R-, *Genista scorpius*) in blue, a resprouting shrub (R+, *Quercus coccifera*) in purple and a tree (Tr, *Quercus ilex*) in green, in a representative sampling location (*AraCin12*). Error bars indicate standard error.

amongst others plant traits, inter-specific and seasonal differences. Importantly, we were able to realistically capture seasonal variations (Fig. A3) in LFMF across individuals belonging to different species (Fig. 3), genus (Table 2) and functional types (Fig. 2), and, overall, we demonstrated that our approach had a higher predictive ability than approaches based on remotely sensed spectral vegetation indices or drought indices (Table 1, Fig. 2).

Our $MEDFATE_{LFMC}$ model was able to realistically capture the temporal patterns of variation in LFMF across functional types. Following expectations, species with shallower root systems, such as seeding shrubs, showed faster LFMF reductions during the summer dry period (Fig. 3). On the other hand, tree species with deeper root systems were less responsive to seasonal dryness, showing relatively little seasonal variation in LFMF, consistent with their larger dependence on deep soil water pools. Finally, resprouting shrub species show an intermediate dependence on shallow and deep water pools between seeding shrubs and tree species, resulting in an intermediate level of seasonal LFMF variation (Nolan et al., 2018).

We observed a better performance for modelling LFMF in seeding shrubs and trees than for resprouting shrubs. This may be due to a lack of temporal continuity in resprouting shrub records at most sampling sites, as there were only two sites with more than three consecutive weekly measurements. Temporal discontinuity in the data can in turn decrease model performance due to poor data quality (Quan et al., 2021). Another possibility for a poorer model performance in resprouters could be the smaller temporal variation in LFMF records. At any rate, our method for predicting LFMF in resprouters presents a significant improvement over existing commonly used approaches based on optical remote sensing and drought indices (Fig. 2).

It is likely that LFMF predictions from our approach could be

improved further by a more realistic description of the factors creating temporal variation as well as differences across species. Further studies using our model may derive LFMF from Ψ_{pd} as presented here (Fig. A2), but they are encouraged to develop their own calibration, particularly if dealing with very different vegetation types. Also, it is important that future studies consider the possibility of using species-specific pressure-volume curves to obtain LFMF estimates from Ψ_{pd} (Nolan et al., 2020) to understand whether better predictions may be obtained.

LFMF depends on water content relative to dry mass (Pimont et al., 2019), consequently, the incorporation of processes affecting dry mass may lead to further improvements (Jolly et al., 2014). Seasonal changes in specific leaf area, for instance, may alter maximum LFMF (Nolan et al., 2020). Similarly, differences in specific leaf area across species are likely to alter the relationship between LFMF and Ψ_{pd} . That is, at a given water potential (or water content), we can expect higher LFMF in species with larger specific leaf area because dry matter content will be lower. A more realistic description of rooting depth may also be achieved by coupling species-specific root depth models (Cabon et al., 2018). However, we chose not to incorporate these variables in the current study because we sought to develop a relatively simple model that could be easily regionalised to work at national scales within operational settings. Further research could address to which extent model predictions could be improved by incorporating phenological as well as inter-specific differences in dry mass and rooting depth.

We observed that DC provided reliable LFMF predictions for seeding shrubs, but not for trees or resprouting shrubs species (Fig. 2). In the case of EVI, we always observed a poor relationship with EWT. LFMF varies over longer time-scales than the period between two consecutive MODIS measurements (Pellizzaro et al., 2007a; Resco de Dios et al., 2021; Viegas et al., 2001). The slight temporal mismatch between LFMF and

MODIS measurements is thus unlikely to significantly affect the results. Our goal was to develop a species-specific model, and, to that end, our approach showed a superior performance, allowing, for example, to model understory and overstory species separately, while remotely sensed models typically provide an integrated estimate. It is likely that EVI computed from remotely sensed imagery with higher spatial (i.e., Sentinel 3), will show a stronger relationship with species-specific LFMC values than the one shown here, but as it is an empirical approach, predictive capabilities would continue to be limited. However, we used MODIS instead as it has a longer coverage for model validation and overlap with the Globe-LFMC data set. It is worth noting that recent developments in the field of remote sensed Vegetation Optical Depth to detect vegetation response to water stress, also allow for enhanced realism in LFMC predictions (Rao et al., 2020). Understanding the potential for high resolution satellites remote sensed Vegetation Optical Depth approaches in monitoring species-specific variations in LFMC is another topic for future development.

Despite the large amount of input data required to run MEDFATE simulations (Table A1), much of the complexities of state variables and parameters can be hidden from the user in practical operational tools. Our approach can be implemented within large scale fire danger forecast systems and may pave the way for a new generation of process-based models that are used for operational purposes within fire prevention scenarios.

5. Conclusions

We have developed an approach to predict LFMC by combining a process-based model for the estimation of Ψ_{pd} and an empirical relationship between Ψ_{pd} and LFMC that allows predictions of species-specific seasonal changes and forecasts of future flammability conditions. Our predictions show better agreement with observed LFMC than drought indices or vegetation indices, not only in general terms, but also by species functional types and genus. Our approach can be implemented within large scale fire danger forecast systems and may pave the way for a new generation of process-based models that are used for operational purposes within fire prevention scenarios. As moisture is a critical driver of fire behaviour and considering the projected increases in extreme fire weather events, we suggest the incorporation of plant physiological traits and process-based eco-hydrological models to better constrain fire behaviour projections, and also to better understand fuel availability dynamics for improving fire prevention actions.

Funding

This work was partly funded by the Spanish Government, grant number RTI2018-094691-B-C31 (MCIU/AEI/FEDER, EU). R.B.-R. acknowledges the Community of Madrid for the predoctoral contract PEJD-2019-PRE/AMB-15,644 funded by the Youth Employment Initiative (YEI). M. De C. was supported by the Spanish Ministry of Science and Innovation via competitive grant CGL2017-89149-C2-2-R. UNED funding for open access publishing.

Declaration of Competing Interest

The authors declare that they have no known competing financial interests or personal relationships that could have appeared to influence the work reported in this paper.

Supplementary materials

Supplementary material associated with this article can be found, in the online version, at doi:10.1016/j.agrformet.2022.109022.

References

- Alberdi, I., Sandoval, V., Condes, S., Cañellas, I., Vallejo, R., 2016. The Spanish National Forest Inventory, a tool for the knowledge, management and conservation of forest ecosystems. *Ecosistemas* 25, 88–97. <https://doi.org/10.7818/ecos.2016.25-3.10>.
- Balaguer-Romano, R., Díaz-Sierra, R., Madrigal, J., Voltas, J., de Dios, V.R., 2020. Needle senescence affects fire behavior in Aleppo pine (*Pinus halepensis* mill.) stands: a simulation study. *Forests*. <https://doi.org/10.3390/f11101054>.
- Boer, M.M., De Dios, V.R., Stefaniak, E.Z., Bradstock, R.A., 2021. A hydroclimatic model for the distribution of fire on earth. *Environ. Res. Commun.* 3 <https://doi.org/10.1088/2515-7620/abec1f>.
- Borchers-Arriagada, N., Bowman, D.M.J.S., Price, O., Palmer, A.J., Samson, S., Clarke, H., Sepulveda, G., Johnston, F.H., 2021. Smoke health costs and the calculus for wildfires fuel management: a modelling study. *Lancet Planet. Health* 5, e608–e619. [https://doi.org/10.1016/s2542-5196\(21\)00198-4](https://doi.org/10.1016/s2542-5196(21)00198-4).
- Cabon, A., Martínez-Vilalta, J., Martínez de Aragón, J., Poyatos, R., De Cáceres, M., 2018. Applying the eco-hydrological equilibrium hypothesis to model root distribution in water-limited forests. *Ecohydrology* 11. <https://doi.org/10.1002/eco.2015>.
- Chakroun, H., Mouillot, F., Hamdi, A., 2015. Regional Equivalent Water Thickness Modeling from Remote Sensing Across a Tree Cover/LAI Gradient in Mediterranean Forests of Northern Tunisia 1937–1961. <https://doi.org/10.3390/rs70201937>.
- Chazarra Bernabé, A., Flórez García, E., Peraza Sánchez, B., Tohá Rebull, T., Lorenzo Mariño, B., Criado Pinto, E., Moreno García, J.V., Romero Fresneda, R., Botey Fullat, R., 2018. Mapas climáticos de España (1981-2010) y ETo (1996-2016), Mapas climáticos de España (1981-2010) y ETo (1996-2016). Agencia Estatal de Meteorología. <https://doi.org/10.31978/014-18-004-2>.
- Davidson, R., MacKinnon, J., 1993. *Estimation and Inference in Econometrics*. New York.
- De Cáceres, M., Martín-StPaul, N., Turco, M., Cabon, A., Granda, V., 2018. Estimating daily meteorological data and downscaling climate models over landscapes. *Environ. Model. Softw.* 108, 186–196. <https://doi.org/10.1016/j.envsoft.2018.08.003>.
- De Cáceres, M., Martínez-Vilalta, J., Coll, L., Llorens, P., Casals, P., Poyatos, R., Pausas, J. G., Brotons, L., 2015. Coupling a water balance model with forest inventory data to predict drought stress: the role of forest structural changes vs. climate changes. *Agric. For. Meteorol.* 213, 77–90. <https://doi.org/10.1016/j.agrformet.2015.06.012>.
- De Cáceres, M., Mencuccini, M., Martín-StPaul, N., Limousin, J.M., Coll, L., Poyatos, R., Cabon, A., Granda, V., Forner, A., Valladares, F., Martínez-Vilalta, J., 2021. Unravelling the effect of species mixing on water use and drought stress in Mediterranean forests: a modelling approach. *Agric. For. Meteorol.* 296 <https://doi.org/10.1016/j.agrformet.2020.108233>.
- Dinerstein, E., Olson, D., Joshi, A., Vynne, C., Burgess, N.D., Wikramanayake, E., Hahn, N., Palminteri, S., Hedao, P., Noss, R., Hansen, M., Locke, H., Ellis, E.C., Jones, B., Barber, C.V., Hayes, R., Kormos, C., Martin, V., Crist, E., Sechrest, W., Price, L., Baillie, J.E.M., Weeden, D., Suckling, K., Davis, C., Sizer, N., Moore, R., Thau, D., Birch, T., Potapov, P., Turubanova, S., Tyukavina, A., De Souza, N., Pintea, L., Brito, J.C., Llewellyn, O.A., Miller, A.G., Patzelt, A., Ghazanfar, S.A., Timberlake, J., Klöser, H., Shennan-Farpon, Y., Kindt, R., Lilleso, J.P.B., Van Breugel, P., Graudal, L., Voge, M., Al-Shammari, K.F., Saleem, M., 2017. An ecoregion-based approach to protecting half the terrestrial realm. *Bioscience* 67, 534–545. <https://doi.org/10.1093/biosci/bix014>.
- Duane, A., Castellnou, M., Brotons, L., 2021. Towards a comprehensive look at global drivers of novel extreme wildfire events. *Clim. Change* 165, 1–21. <https://doi.org/10.1007/s10584-021-03066-4>.
- Gabriel, E., Delgado-Dávila, R., De Cáceres, M., Casals, P., Tudela, A., Castro, X., 2021. Live fuel moisture content time series in Catalonia since 1998. *Ann. For. Sci.* 78 <https://doi.org/10.1007/s13595-021-01057-0>.
- Granier, A., Bréda, N., Biron, P., Villette, S., 1999. A lumped water balance model to evaluate duration and intensity of drought constraints in forest stands. *Ecol. Modell.* 116, 269–283. [https://doi.org/10.1016/S0304-3800\(98\)00205-1](https://doi.org/10.1016/S0304-3800(98)00205-1).
- Hengl, T., Jesus, J.M.De, Heuvelink, G.B.M., Ruiperez, M., Kilibarda, M., Blagoti, A., Shangguan, W., Wright, M.N., Geng, X., Bauer-marschallinger, B., Guevara, M.A., Vargas, R., Macmillan, R.A., Batjes, N.H., Leenaars, J.G.B., Ribeiro, E., Wheeler, I., Mantel, S., Kempen, B., 2017. SoilGrids250m: global gridded soil information based on machine learning. <https://doi.org/10.1371/journal.pone.0169748>.
- Hersbach, H., Bell, B., Berrisford, P., Hirahara, S., Horányi, A., Muñoz-Sabater, J., Nicolas, J., Peubey, C., Radu, R., Schepers, D., Simmons, A., Soci, C., Abdalla, S., Abellan, X., Balsamo, G., Bechtold, P., Biavati, G., Bidlot, J., Bonavita, M., De Chiara, G., Dahlgren, P., Dee, D., Diamantakis, M., Dragani, R., Flemming, J., Forbes, R., Fuentes, M., Geer, A., Haimberger, L., Healy, S., Hogan, R.J., Hólm, E., Janisková, M., Keeley, S., Laloyaux, P., Lopez, P., Lupu, C., Radnoti, G., de Rosnay, P., Rozum, I., Vamborg, F., Villaume, S., Thépaut, J.N., 2020. The ERA5 global reanalysis. *Q. J. R. Meteorol. Soc.* 146, 1999–2049. <https://doi.org/10.1002/qj.3803>.
- IPCC, 2021. *Climate Change 2021: The Physical Science Basis. Contribution of Working Group I to the Sixth Assessment Report of the Intergovernmental Panel on Climate Change*. Cambridge University Press.
- Jolliffe, J.K., Kindle, J.C., Shulman, I., Penta, B., Friedrichs, M.A.M., Helber, R., Arnone, R.A., 2009. Summary diagrams for coupled hydrodynamic-ecosystem model skill assessment. *J. Mar. Syst.* 76, 64–82. <https://doi.org/10.1016/j.jmarsys.2008.05.014>.
- Jolly, W.M., Hadlow, A.M., Hugué, K., 2014. De-coupling seasonal changes in water content and dry matter to predict live conifer foliar moisture content. *Int. J. Wildl. Fire* 23, 480–489. <https://doi.org/10.1071/WF13127>.

- Jurdao, S., Chuvieco, E., Arealillo, J.M., 2012. Modelling fire ignition probability from satellite estimates of live fuel moisture content. *Fire Ecol.* 8, 77–97. <https://doi.org/10.4996/fireecology.0801077>.
- Karavani, A., Boer, M.M., Baudena, M., Colinas, C., Díaz-Sierra, R., Pemán, J., de Luis, M., Enríquez-de-Salamanca, A., Resco de Dios, V., 2018. Fire-induced deforestation in drought-prone Mediterranean forests: drivers and unknowns from leaves to communities. *Ecol. Monogr.* 88, 141–169. <https://doi.org/10.1002/ecm.1285>.
- Luo, K., Quan, X., He, B., Yebra, M., 2019. Effects of live fuel moisture content on wildfire occurrence in fire-prone regions over southwest China. *Forests* 10, 1–17. <https://doi.org/10.3390/f10100887>.
- Ma, W., Zhai, L., Pivovarov, A., Shuman, J., Buotte, P., Ding, J., Christoffersen, B., Knox, R., Moritz, M., Fisher, R.A., Koven, C.D., Kueppers, L., Xu, C., 2021. Assessing climate change impacts on live fuel moisture and wildfire risk using a hydrodynamic vegetation model. *Biogeosciences* 18, 4005–4020. <https://doi.org/10.5194/bg-18-4005-2021>.
- Marino, E., Yebra, M., Guill, M., Algeet, N., Tom, L., Madrigal, J., Guijarro, M., Hernando, C., 2020. Investigating live fuel moisture content estimation in fire-prone shrubland from remote sensing using empirical modelling and RTM simulations. *Remote Sens.* 12.
- Matthews, S., 2014. Dead fuel moisture research: 1991–2012. *Int. J. Wildl. Fire* 23, 78–92. <https://doi.org/10.1071/WF13005>.
- McDonald, M., 2020. After the fires? Climate change and security in Australia. *Aust. J. Polit. Sci.* 56, 1–18. <https://doi.org/10.1080/10361146.2020.1776680>.
- Moreno-Gutiérrez, C., Barberá, G.G., Nicolás, E., De Luis, M., Castillo, V.M., Martínez-Fernández, F., Querejeta, J.L., 2011. Leaf δ18O of remaining trees is affected by thinning intensity in a semiarid pine forest. *Plant Cell Environ.* 34, 1009–1019. <https://doi.org/10.1111/j.1365-3040.2011.02300.x>.
- Mouillot, F., Rambal, S., Lavorel, S., 2001. A generic process-based simulator for mediterranean landscapes (SIERRA): design and validation exercises. *For. Ecol. Manag.* 147, 75–97. [https://doi.org/10.1016/S0378-1127\(00\)00432-1](https://doi.org/10.1016/S0378-1127(00)00432-1).
- Nolan, R.H., Blackman, C.J., Dios, R.De, Choat, B., Medlyn, B.E., Li, X., Bradstock, R.A., Boer, M.M., 2020. Linking forest flammability and plant vulnerability to drought. *Forests* 1–16.
- Nolan, R.H., Boer, M.M., Resco De Dios, V., Caccamo, G., Bradstock, R.A., 2016. Large-scale, dynamic transformations in fuel moisture drive wildfire activity across southeastern Australia. *Geophys. Res. Lett.* 43, 4229–4238. <https://doi.org/10.1002/2016GL068614>.
- Nolan, R.H., Hedo, J., Arteaga, C., Sugai, T., Resco de Dios, V., 2018. Physiological drought responses improve predictions of live fuel moisture dynamics in a Mediterranean forest. *Agric. For. Meteorol.* 263, 417–427. <https://doi.org/10.1016/j.agrformet.2018.09.011>.
- Pausas, J.G., Pratt, R.B., Keeley, J.E., Jacobsen, A.L., Ramirez, A.R., Vilagrosa, A., Paula, S., Kaneakua-Pia, I.N., Davis, S.D., 2016. Towards understanding resprouting at the global scale. *New Phytol.* 209, 945–954. <https://doi.org/10.1111/nph.13644>.
- Pellizzaro, G., Cesaraccio, C., Duce, P., Ventura, A., Zara, P., 2007a. Relationships between seasonal patterns of live fuel moisture and meteorological drought indices for Mediterranean shrubland species. *Int. J. Wildl. Fire* 16, 232–241. <https://doi.org/10.1071/WF06081>.
- Pellizzaro, G., Duce, P., Ventura, A., Zara, P., 2007b. Seasonal variations of live moisture content and ignitability in shrubs of the Mediterranean Basin. *Int. J. Wildl. Fire* 16, 633–641. <https://doi.org/10.1071/WF05088>.
- Pimont, F., Ruffault, J., Martin-StPaul, N.K., Dupuy, J.L., 2019. Why is the effect of live fuel moisture content on fire rate of spread underestimated in field experiments in shrublands? *Int. J. Wildl. Fire* 28, 127–137. <https://doi.org/10.1071/WF18091>.
- Quan, X., Yebra, M., Riaño, D., He, B., Lai, G., Liu, X., 2021. Global fuel moisture content mapping from MODIS. *Int. J. Appl. Earth Obs. Geoinf.* 101, 102354. <https://doi.org/10.1016/j.jag.2021.102354>.
- Rao, K., Williams, A.P., Flefil, J.F., Konings, A.G., 2020. SAR-enhanced mapping of live fuel moisture content. *Remote Sens. Environ.* 245, 111797. <https://doi.org/10.1016/j.rse.2020.111797>.
- Resco de Dios, V., 2020. *Plant-Fire Interactions*, Managing F. ed. Springer US, Switzerland.
- Resco de Dios, V., Hedo, J., Cunill, À., Thapa, P., Martínez, E., Martínez, J., Aragón, D., Antonio, J., Balaguer-Romano, R., Díaz-sierra, R., Yebra, M., Boer, M.M., 2021. Climate change induced declines in fuel moisture may turn currently fire-free Pyrenean mountain forests into fire-prone ecosystems. *Sci. Total Environ.* 797, 149104. <https://doi.org/10.1016/j.scitotenv.2021.149104>.
- Resco de Dios, V., Nolan, R.H., 2021. Some challenges for forest fire risk predictions in the 21st century. *Forests* 12, 1–5. <https://doi.org/10.3390/f12040469>.
- Ritchie, G.A., Hinckley, T.M., 1975. The pressure chamber as an instrument for ecological research. *Adv. Ecol. Res.* 9, 165–254. [https://doi.org/10.1016/S0065-2504\(08\)60290-1](https://doi.org/10.1016/S0065-2504(08)60290-1).
- Rossa, C.G., 2017. The effect of fuel moisture content on the spread rate of forest fires in the absence of wind or slope. *Int. J. Wildl. Fire* 26, 24–31. <https://doi.org/10.1071/WF16049>.
- Rothermel, R.C., 1983. How to predict the spread and intensity of forest and range fires. US Dep. Agric. For. Serv. Gen. Tech. Rep. <https://doi.org/10.2737/INT-GTR-143>.
- Ruffault, J., Martin-StPaul, N., Pimont, F., Dupuy, J.L., 2018. How well do meteorological drought indices predict live fuel moisture content (LFMC)? An assessment for wildfire research and operations in Mediterranean ecosystems. *Agric. For. Meteorol.* 262, 391–401. <https://doi.org/10.1016/j.agrformet.2018.07.031>.
- Sanchez-Martinez, P., Martínez-Vilalta, J., Dexter, K.G., Segovia, R.A., Mencuccini, M., 2020. Adaptation and coordinated evolution of plant hydraulic traits. *Ecol. Lett.* 23, 1599–1610. <https://doi.org/10.1111/ele.13584>.
- Soler Martin, M., Bonet, J.A., Martínez De Aragón, J., Voltas, J., Coll, L., Resco De Dios, V., 2017. Crown bulk density and fuel moisture dynamics in Pinus pinaster stands are neither modified by thinning nor captured by the Forest Fire Weather Index. *Ann. For. Sci.* 74. <https://doi.org/10.1007/s13595-017-0650-1>.
- Sow, M., Mbow, C., Hély, C., Fensholt, R., Sambou, B., 2013. Estimation of herbaceous fuel moisture content using vegetation indices and land surface temperature from MODIS data. *Remote Sens.* 2617–2638. <https://doi.org/10.3390/rs5062617>.
- Sperry, J.S., Venturas, M.D., Anderegg, W.R.L., Mencuccini, M., Mackay, D.S., Wang, Y., Love, D.M., 2017. Predicting stomatal responses to the environment from the optimization of photosynthetic gain and hydraulic cost. *Plant Cell Environ.* 40, 816–830. <https://doi.org/10.1111/pce.12852>.
- Tedim, F., Leone, V., Mcgee, T., 2020. *Extreme Wildfire Events and Disasters: Root Causes and New Management Strategies*. Elsevier, Amsterdam, Netherlands.
- Thornton, P.E., Running, S.W., 1999. An Improved Algorithm for Estimating Incident Daily Solar Radiation from Measurements of temperature, humidity, and Precipitation, p. 93.
- Van Wagner, C.E., 1974. Structure of the Canadian forest fire weather index. *Dep. Environ. - Can. For. Serv. Publ.* 37 pp.
- Viegas, D.X., Piñol, J., Viegas, M.T., Ogaya, R., 2001. Estimating live fine fuels moisture content using meteorologically-based indices. *Int. J. Wildl. Fire* 10, 223–240. <https://doi.org/10.1071/WF01022>.
- Wang, X., Wotton, B.M., Cantin, A.S., Parisien, M.A., Anderson, K., Moore, B., Flannigan, M.D., 2017. cffdrs: an R package for the Canadian Forest fire danger rating system. *Ecol. Process.* 6. <https://doi.org/10.1186/s13717-017-0070-z>.
- Yebra, M., Dennison, P.E., Chuvieco, E., Riaño, D., Zylstra, P., Hunt, E.R., Danson, F.M., Qi, Y., Jurdao, S., 2013. A global review of remote sensing of live fuel moisture content for fire danger assessment: moving towards operational products. *Remote Sens. Environ.* 136, 455–468. <https://doi.org/10.1016/j.rse.2013.05.029>.
- Yebra, M., Scortechini, G., Badi, A., Beget, M.E., Boer, M.M., Bradstock, R., Chuvieco, E., Danson, F.M., Dennison, P., Resco de Dios, V., Di Bella, C.M., Forsyth, G., Frost, P., Garcia, M., Hamdi, A., He, B., Jolly, M., Kraaij, T., Martín, M.P., Mouillot, F., Newnham, G., Nolan, R.H., Pellizzaro, G., Qi, Y., Quan, X., Riaño, D., Roberts, D., Sow, M., Ustin, S., 2019. Globe-LFMC, a global plant water status database for vegetation ecophysiology and wildfire applications. *Sci. Data* 6, 1–8. <https://doi.org/10.1038/s41597-019-0164-9>.
- Zeileis, A., Hothorn, T., 2002. Diagnostic Checking in Regression Relationships, 2. R News, pp. 7–10.